World Applied Sciences Journal 33 (3): 525-535, 2015
ISSN 1818-4952

DOI: 10.5829/idosi.wasj.2015.33.03.14576

Dynamic Optimization of Thin-walled Composite Blades of Wind Turbines

[1]G.E. Beshay, [2]K.Y. Maalawi, [1]S.M. Abdrabbo and [1]T.A. Khalifa

[1]Department of Mechanical Engineering, Faculty of Engineering (Shoubra), Benha University, Cairo, Egypt
[2]Department of Mechanical Engineering, National Research Centre, Dokki, Giza, Egypt

Abstract: The design of thin-walled composite blades is optimized in order to provide high dynamic performance. The optimal design is originated with respect to maximum natural frequency criterion. The optimization model employs the concept of spanwise material grading along the blade axis. Spanwise material grading is achieved by changing the distribution of fiber volume fraction along the blade length. The main blade spar is represented by a beam composed of multiple uniform segments each of which has different cross-sectional properties and length. Transfer matrix technique is used to study the dynamic behavior of such a beam. Design variables are chosen to be the cross-section dimensions, length, fiber orientation angle and fiber volume fraction of each segment. The optimization problem is formulated analytically as non-linear constrained problem solved by sequential quadratic programming technique. Finite element modeling using NX Nastran solver is performed in order to validate the analytical results. The results show that the approach used in this study enhances the dynamic characteristics of the optimized blades as compared with a baseline design.

Key words: Dynamic optimization . natural frequencies . fiber composites . functionally graded materials . thin-walled blades

INTRODUCTION

Thin-walled composite beams with a variety of cross sections are used extensively in the design of many aerodynamic structures. Applications such as wind turbines, aircraft propellers and helicopter rotor blades mainly built up of thin-walled composite beams [1, 2]. To design these components, the dynamic characteristic, especially near resonant conditions, need to be well examined to assure a safe operation. Among the dynamic characteristics of these structures, determination of the natural frequencies and the associated mode shapes are of fundamental importance. The objective of this investigation is to optimize the structural dynamics of a thin-walled composite blade through the reduction of the overall vibration level. The latter can be attained directly by maximizing the natural frequencies of the main blade structure under strength and mass constraints. In general conditions however we need a material that is as light as possible for a specified stiffness in order to satisfy the design criteria and to minimize the weight induced fatigue loads. Composite materials offer huge advantages in terms of strength-to-weight ratios [3]. The main advantages of fiber composite materials are their high strength and stiffness combined with low density, their superior fatigue properties due to the prevention of crack propagation and the ability to tailor the layup for optimum strength and stiffness. However, sharp transitions between component materials may cause stress and strain discontinuities that facilitate failure [4]. A solution that can be promising to enhance dynamic stability of composite blades is the use of functionally graded materials (FGMs), in which the mechanical and physical properties vary spatially within the structure [5]. A functionally graded material is a material in which the composition and/or the structure gradually change resulting in a corresponding change in its properties [6].

Analytical model for the free vibration of anisotropic thin-walled closed-section uniform beams was developed by Armanios and Badir [7] using a variational asymptotic approach and Hamilton's principles. This model is applied to uniform thin-walled beams with arbitrary closed cross sections made of laminated fiber composite materials with variable thickness and stiffness. The analysis was applied to two kinds of laminated composites: Circumferentially Uniform Stiffness (CUS) and Circumferentially Asymmetric Stiffness (CAS). The model developed by Armanios and Badir was used by Dancila and Armanios [8] to study the influence of coupling on the free

Corresponding Author: G.E. Beshay, Department of Mechanical Engineering, Faculty of Engineering (Shoubra), Benha University, Cairo, Egypt

vibration of thin-walled composite beams. The model was also used by Durmaz and Kaya [9] to study the free vibration of thin-walled box beams in the case of bending-torsion coupling. The static and dynamic characteristics of composite thin-walled beams that are constructed from a single cell were considered by Shadmehri et al. [10]. The structural model considered incorporated a number of non-classical effects, such as material anisotropy, transverse shear, warping inhibition, non-uniform torsion and rotary inertia. The governing equations were derived using extended Hamilton's principle and solved using extended Galerkin's method. Phuong and Lee [11] presented a flexural–torsional analysis of thin-walled composite box beams. A general analytical model applicable to thin-walled composite box beams subjected to vertical and torsional loads was developed. Piovan et al. [12] developed analytical solutions for the free vibration analysis of tapered thin-walled laminated-composite beams with closed cross-sections. The exact values of frequencies were obtained by means of power series schemes. A parametric analysis was performed for different taper ratios, stacking sequences and materials. Kargarnovin and Hashemi [13] investigated the free vibration of a fiber composite cylinder, in which volume fraction of fibers vary longitudinally, using a semi-analytical method. The distribution of volume fraction of fiber in base matrix was based on power law model. Liu and Shu [14] developed an analytical solution to study the free vibration of exponential functionally graded beams with a single delamination. They showed that the natural frequencies increase as Young's modulus ratio becomes bigger.

In the present study, an analytical model is developed to study the dynamic behavior of tapered thin-walled composite blades using transfer matrix technique. Furthermore, the main blade structure is optimized using material grading concept in order to maximize its natural frequencies without mass penalty.

Kinematic variables and constitutive equations: Considering a closed-section composite shell illustrated in Fig. 1. The length of the shell is denoted by L, its thickness by h, the radius of curvature of the middle surface by R and the maximum cross section dimension by d such that:

$$\begin{matrix} d<<L \\ h<<d \\ h<<R \end{matrix} \qquad (1)$$

Following the methodology given by Armanios and Badi [7], the constitutive relationships can be written in terms of stress resultants and kinematic variables as follows:

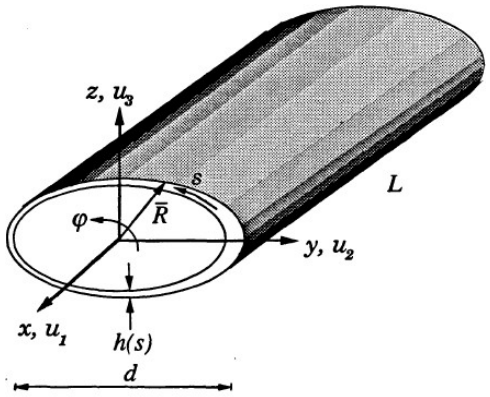

Fig. 1: Closed-section shell with arbitrary shape [7]

$$\begin{bmatrix} T \\ M_x \\ M_y \\ M_z \end{bmatrix} = \begin{bmatrix} C_{11} & C_{12} & C_{13} & C_{14} \\ C_{12} & C_{22} & C_{23} & C_{24} \\ C_{13} & C_{23} & C_{33} & C_{34} \\ C_{14} & C_{24} & C_{34} & C_{44} \end{bmatrix} \begin{bmatrix} U_1' \\ \varphi'' \\ U_3'' \\ U_2'' \end{bmatrix} \qquad (2)$$

where, T is the traction force, M_x is the torsional moment, M_y and M_z are flexural moments about y and z axes respectively and C_{ij} the cross sectional stiffness coefficients. Four global kinematic variables are defined at a cross sectional level: U_1, U_2 and U_3 are the average cross sectional displacements in x, y and z directions respectively and φ is the cross sectional twist function about x-axis. The prime superscripts indicate differentiations with respect to x.

General equations of motion: The equations of motion for the case of undamped free vibration are obtained using Hamilton's principle [7], as follows:

$$\begin{aligned} &C_{11}U_1'' + C_{12}\varphi'' + C_{13}U_3''' + C_{14}U_2''' - m_c\ddot{U}_1 = 0 \\ &C_{12}U_1'' + C_{22}\varphi'' + C_{23}U_3''' + C_{24}U_2''' - I\ddot{\varphi} - S_z\ddot{U}_3 + S_y\ddot{U}_2 = 0 \\ &C_{13}U_1''' + C_{23}\varphi''' + C_{33}U_3'''' + C_{34}U_2'''' + S_z\ddot{\varphi} + m_c\ddot{U}_3 = 0 \\ &C_{14}U_1''' + C_{24}\varphi''' + C_{34}U_3'''' + C_{44}U_2'''' - S_y\ddot{\varphi} + m_c\ddot{U}_2 = 0 \end{aligned} \qquad (3)$$

where, m_c is the mass per unit length of the beam, I is the polar moment of inertia per unit length, S_z and S_y are the first moment of inertia per unit length about z and y axes respectively. The dot superscripts denote differentiation with respect to time. Detailed derivations for calculating the cross sectional stiffness coefficients are given by Armanios and Badir [7]. The reduced axial, coupled axial-shear and shear stiffness coefficients of a thin-walled composite laminate are, respectively, given by:

$$A = A_{11} - (A_{12})^2 / A_{22}$$
$$B = 2[A_{16} - A_{12}A_{26} / A_{22}] \quad (4)$$
$$C = 4[A_{66} - (A_{26})^2 / A_{22}]$$

where, A_{ij} are the membrane in-plane stiffnesses given by Berthelot [3]:

$$A_{ij} = \sum_{k=1}^{n} \overline{Q}_{ijk}(z_k - z_{k-1}) \qquad i,j = 1,2,6 \quad (5)$$

where, z_k and z_{k-1} are the upper and lower coordinate of the k^{th} ply within the laminate. $\overline{Q}_{ijk}$ are the elements of the k^{th} lamina stiffness matrix referred to the reference axes (x, y, z) and they are given by Reddy [15]:

$$\overline{Q}_{11} = H_1 + H_2\cos 2\theta + H_3\cos 4\theta$$
$$\overline{Q}_{22} = H_1 - H_2\cos 2\theta + H_3\cos 4\theta$$
$$\overline{Q}_{12} = H_4 - H_3\cos 4\theta \quad (6)$$
$$\overline{Q}_{16} = 0.5H_2\sin 2\theta + H_3\sin 4\theta$$
$$\overline{Q}_{26} = 0.5H_2\sin 2\theta - H_3\sin 4\theta$$
$$\overline{Q}_{66} = 0.5(H_1 - H_4) - H_3\cos 4\theta$$

where,

$$H_1 = (3Q_{11} + 3Q_{22} + 2Q_{12} + 4Q_{66})/8$$
$$H_2 = (Q_{11} - Q_{22})/2 \quad (7)$$
$$H_3 = (Q_{11} + Q_{22} - 2Q_{12} - 4Q_{66})/8$$
$$H_4 = (Q_{11} + Q_{22} + 6Q_{12} - 4Q_{66})/8$$

where, θ is the fiber orientation angle within each lamina with respect to the x-axis. Q_{ij} are the elements of the stiffness matrix of the reduced form of Hooke's law for an orthotropic homogeneous lamina in a plane stress state and they are given by Daneil and Ishai [2]:

$$Q_{11} = E_{11}/(1 - \nu_{12}^2 E_{22}/E_{11})$$
$$Q_{22} = E_{22}/(1 - \nu_{12}^2 E_{22}/E_{11}) \quad (8)$$
$$Q_{12} = \nu_{12}E_{22}/(1 - \nu_{12}^2 E_{22}/E_{11})$$
$$Q_{66} = G_{12}$$

where, E_{11} and E_{22} are the Young's moduli in the longitudinal and lateral directions of the lamina, G_{12} is the shear modulus and ν_{12} is the major Poisson's ratio. Based upon the semi-empirical methods by Halpin and Tsai [16], they are given by:

$$E_{11} = E_m(1 - V_f) + E_f V_f$$
$$E_{22} = E_m(1 + \eta_E V_f)/(1 - \eta_E V_f)$$
$$G_{12} = G_m(1 + \eta_G V_f)/(1 - \eta_G V_f)$$
$$\nu_{12} = \nu_m(1 - V_f) + \nu_f V_f$$

$$\eta_E = (E_f - E_m)/(E_f + E_m)$$
$$\eta_G = (G_f - G_m)/(G_f + G_m) \quad (9)$$

Subscripts "m" and "f" refer to properties of matrix and fiber materials respectively. V_f is the volume fraction of fibers within each lamina.

Particular case studies: Two particular cases of fiber layup are considered in which some of stiffness coefficients vanish: circumferentially uniform stiffness (CUS) and Circumferentially Asymmetric Stiffness (CAS) [17]. The cross section of the beam under consideration is selected to be rectangular for its wide applications in aerodynamic structures. Figure 2 shows a rectangular box beam with both CUS and CAS layup configurations. For a CUS layup configuration, the stiffness coefficients A, B and C are constant throughout the cross section. While, for a CAS layup configuration, the axial stiffness A is constant throughout the cross section, while the coupled axial-shear stiffness B in the top and bottom members are of opposite sign and the shear stiffness C along the horizontal and vertical members are different ($C_{horizontal} = 0.5C_{vertical}$). For a rectangular box beam with wall thickness t, width w and height h, the governing equations are reduced to:

CUS-layup Configuration

$$C_{11}U_1'' + C_{12}\varphi'' - m_c\ddot{U}_1 = 0$$
$$C_{12}U_1'' + C_{22}\varphi'' - I\ddot{\varphi} = 0 \quad (10)$$
$$C_{33}U_3'' + m_c\ddot{U}_3 = 0$$
$$C_{44}U_2'' + m_c\ddot{U}_2 = 0$$

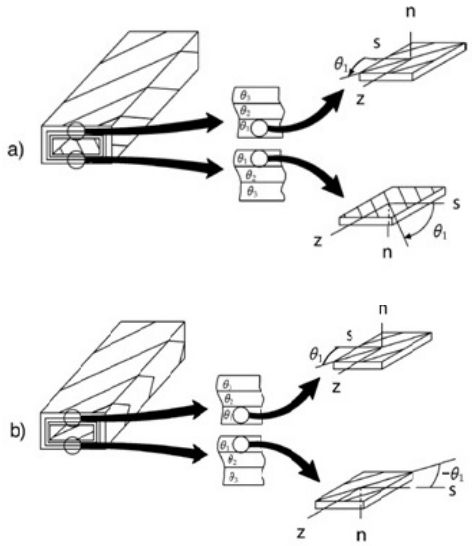

Fig. 2: (a) CUS and (b) CAS layup configurations [17]

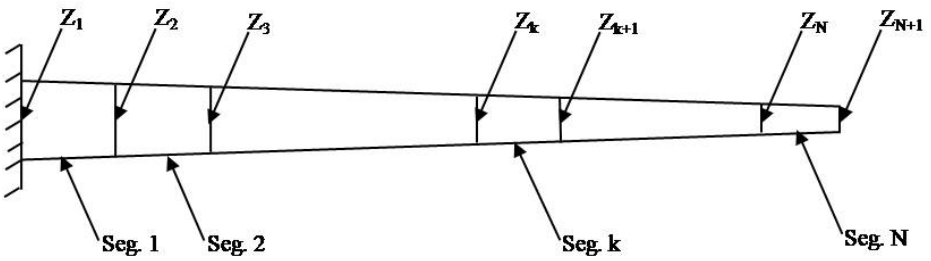

Fig. 3: Modeling of a tapered spar

where

$$
\begin{aligned}
C_{11} &= 2A(w+h-2t)\\
C_{12} &= B(w-t)(h-t)\\
C_{22} &= C\frac{((w-t)(h-t))^2}{2(w+h-2t)}\\
C_{33} &= \left(A-\frac{B^2}{C}\right)\left(\frac{(h-t)^3}{6}\right)\left(1+\frac{3(w-t)}{(h-t)}\right)\\
C_{44} &= \left(A-\frac{B^2}{C}\right)\left(\frac{(w-t)^3}{6}\right)\left(1+\frac{3(h-t)}{(w-t)}\right)
\end{aligned}
\tag{11}
$$

The first two equations of motion are expressing an extension-twist (ET) coupling mode of vibration, while the third and fourth equations of motion are expressing vertical bending (VB) and horizontal bending (HB) modes of vibration, respectively.

CAS layup configuration:

$$
\begin{aligned}
&C_{11}U_1'' - m_c\ddot{U}_1 = 0\\
&C_{22}\varphi'' + C_{23}U_3''' - I\ddot{\varphi} = 0\\
&C_{23}\varphi''' + C_{33}U_3'''' + m_c\ddot{U}_3 = 0\\
&C_{44}U_2'''' + m_c\ddot{U}_2 = 0
\end{aligned}
\tag{12}
$$

where

$$
\begin{aligned}
C_{11} &= 2A(w+h-2t) - 2\frac{B^2}{C}(w-t)\\
C_{22} &= C\frac{((w-t)(h-t))^2}{2((w-t)+(h-t)C/C_v)}\\
C_{23} &= B\frac{((w-t)(h-t))^2}{2((w-t)+(h-t)C/C_v)}\\
C_{33} &= A\frac{(h-t)^3}{6}\left(1+\frac{3(w-t)}{(h-t)}\right)\\
&\quad -\frac{B^2}{2C}\left(1-\frac{(w-t)}{(w-t)+(h-t)C/C_v}\right)(w-t)(h-t)^2
\end{aligned}
$$

$$
C_{44} = \frac{(w-t)^3}{6}\left(\left(1+\frac{3(h-t)}{(w-t)}\right)A-\frac{B^2}{C}\right) \tag{13}
$$

The second and third equations of motion are expressing a coupled vertical bending-twist (BT) mode of vibration, while the first and fourth equations of motion are expressing extension (E) and horizontal bending (HB) modes of vibration, respectively.

Dynamics of a tapered blade spar: Tapered spar can be considered as a beam built up of multiple segments with decreasing cross sectional area as shown in Fig. 3. In order to study the vibratory behavior of such a beam, transfer matrix technique is used [18]. Transfer matrix is a square matrix that relates the state vector at one end of the k^{th} segment Z_k to the state vector at the other end of that segment Z_{k+1}. When considering the flapping motion of the blade, the state vector at the ends of the k^{th} segment can be expressed as:

$$
Z = \begin{bmatrix} \delta_z \\ \phi_y \\ M_y \\ F_z \end{bmatrix} = \begin{bmatrix} U_3 \\ -U_3' \\ -C_{33}U_3'' \\ -C_{33}U_3''' \end{bmatrix} \tag{14}
$$

where, δ_z is the vertical displacement, $\varnothing_y$ is the bending slope, M_y is the bending moment and F_z is the shear force. For a spar beam built up of N-uniform segments:

$$
Z_{N+1} = [T]_o Z_1 \tag{15}
$$

The matrix $[T]_o$ is called the overall transfer matrix formed by taking the products of all the intermediate elementary transfer matrices in the order:

$$
[T]_O = [T]_N [T]_{N-1} \cdots [T]_k \cdots [T]_2 [T]_1 \tag{16}
$$

Therefore, applying the boundary conditions at both ends of the beam and considering only the nontrivial solutions, the frequency equation can be

obtained. As a basic case study, the vertical flapping motion of a beam with CUS layup configuration is considered here. The equation of motion reduces to:

$$C_{33}U_3'''' + m_c\ddot{U}_3 = 0 \tag{17}$$

Its general solution can be expressed as Meirovitch [19]:

$$U_3(x,t) = (c_1\sin\beta x + c_2\cos\beta x + c_3\sinh\beta x + c_4\cosh\beta x)e^{i\omega t} \tag{18}$$

where

$$\beta^2 = \omega\sqrt{m_c / C_{33}}$$

The terms of the elementary transfer matrix $[T]_k$ (Eq. 16) are given by:

$$\begin{aligned}
&T_{11} = T_{22} = T_{33} = T_{44} = (\cos\beta L + \cosh\beta L)/2\\
&T_{12} = -T_{34} = -(\sin\beta L + \sinh\beta L)/(2\beta)\\
&T_{13} = -T_{24} = (\cos\beta L - \cosh\beta L)/(2\beta^2 C_{33})\\
&T_{14} = (\sin\beta L - \sinh\beta L)/(2\beta^3 C_{33})\\
&T_{21} = -T_{43} = \beta(\sin\beta L - \sinh\beta L)/2\\
&T_{23} = (\sin\beta L + \sinh\beta L)/(2\beta C_{33})\\
&T_{31} = -T_{42} = \beta^2 C_{33}(\cos\beta L - \cosh\beta L)/2\\
&T_{32} = -\beta C_{33}(\sin\beta L - \sinh\beta L)/2\\
&T_{41} = -\beta^3 C_{33}(\sin\beta L + \sinh\beta L)/2
\end{aligned} \tag{19}$$

Imposing the cantilevered boundary conditions to the overall beam:

$$\begin{bmatrix}\delta_z\\ \phi_y\\ 0\\ 0\end{bmatrix}_{x=L} = [T]_o \begin{bmatrix}0\\ 0\\ M_y\\ F_z\end{bmatrix}_{x=0} \tag{20}$$

The frequency equation takes the form:

$$T_o(3,3)T_o(4,4) - T_o(3,4)T_o(4,3) = 0 \tag{21}$$

Optimization model formulation: Design Variables: In order to optimize the design of a blade spar with thin-walled rectangular cross section, many geometrical and material variables should be taken into consideration. Geometrical variables are including the spar length (L), width (w), height (h) and wall thickness (t). In this investigation, the aspect ratio of the spar cross section (h/w) is held constant. Composite material variables are including type of constituent materials (fiber and resin), number of laminate layers (nr), fiber volume fraction (V_f), fiber orientation angle (θ) and thickness (d) of each lamina.

Objective function: The objective function is measured by maximizing a weighted sum of successive natural frequencies:

$$f(X) = \sum_{i=1}^{n} w_i\omega_i \tag{22}$$

where, w_i is the weighting factor of the i^{th} natural frequency (ω_i). A reliable way of adjusting the values of the weighting factors can be based on the fact that each frequency is to be maximized from its initial value corresponding to the uniform reference baseline design.

Design constraints:

Constraints imposed on wall thickness of each segment composing the spar beam:

$$\hat{t}_L \le \hat{t}_k \le \hat{t}_U \tag{23}$$

where, $\hat{t}_L$ and $\hat{t}_U$ are lower and upper limits of the non-dimensional wall thicknesses of each segment of the spar ($\hat{t}_k = t_k / t_o$).

Cross-section dimensions of the blade spar: For the k^{th} segment of the blade spar, its height must be less than or equal to the maximum height of the tapered beam corresponding to the segment position. Figure 4 shows the general dimensions of a tapered beam, where "r" and "t" subscripts represent the root and tip locations along the beam.

Maximum height "h_{max}" of any segment within the beam at location "x" is given by:

$$h_{\max} = h_t + x(h_r - h_t)/L_o \tag{24}$$

Typical values of h_r, h_t and L_o considered in this investigation are 250, 50 and 7500 mm, respectively. Lower bounds are also imposed on the height of the k^{th} segment of the beam as a reasonable percentage of the minimum height near the beam tip. Thus, the inequality constraints imposed on the height of each segment of the beam are expressed by:

$$h_{\min} \le h_k \le h_{\max} \tag{25}$$

Constraints imposed on the fiber volume fraction: Fiber volume fraction must be higher than a specific value to insure structural strength and lower than a maximum realistic value from the point view of manufacturing.

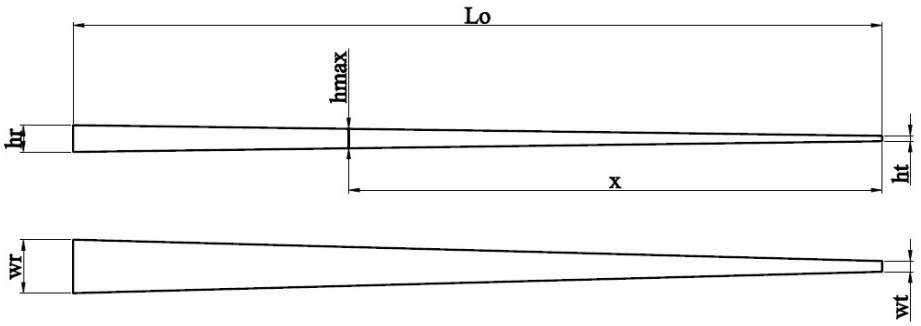

Fig. 4: General dimensions of a tapered spar

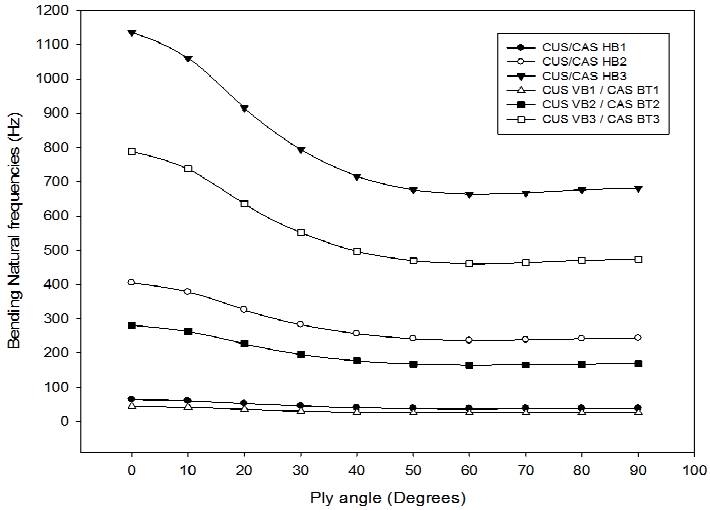

Fig. 5: Effect of fiber angle on horizontal and vertical bending natural frequencies of a single segment cantilevered box beam

$$V_{fL} \le V_f \le V_{fU} \tag{26}$$

Length of the beam: Since the total length of the optimized beam is equal to that of the reference baseline beam, the following equality constraint must be always satisfied:

$$\sum_{k=1}^{ns} \hat{L}_k = 1 \tag{27}$$

Mass constraint: In order not to violate economic feasibility and other performance requirements of a composite blade, an inequality constraint is imposed on the non-dimensional structural mass of the blade spar:

$$(\hat{m} = m / m_o) \le 1 \tag{28}$$

Optimization technique: Sequential Quadratic Programming (SQP) is one of the most recently developed and perhaps one of the best methods of optimization [20]. The method has a theoretical basis that is related to the solution of a set of nonlinear equations using Newton's method and the derivation of simultaneous nonlinear equations using Karush–Kuhn–Tucker (KKT) conditions to the Lagrangian of the constrained optimization problem. The simplest optimization problems are those with quadratic objective function [21]. The essential idea of SQP is to model the optimization problem at the current iterate x_k by a quadratic programming subproblem and to use the minimizer of this subproblem to define a new iterate x_{k+1} [22]. The solution of most practical optimization problems requires the use of computers. Several commercial software systems are available to solve optimization problems that arise in different engineering areas. MATLAB is popular software that is used for the solution of a variety of scientific and engineering problems. MATLAB optimization toolbox contains a library of programs or m-files, which can be used for the solution of optimization problems. The

Table 1: Properties of constituent materials [1]

Property	Epoxy	E-glass
Modulus of elasticity E (GPa)	4.5	74.00
Modulus of rigidity G (GPa)	1.6	30.00
Poisson's ratio	0.4	0.25
Density (kg/m^3)	1200.0	2600.00

Table 2: Natural frequencies of the cantilevered baseline beam

	Natural frequencies (Hz)		
Vibration mode	1st mode	2nd mode	3rd mode
Vertical Bending (VB)	2.80	17.55	49.14
Horizontal Bending (HB)	4.86	30.50	85.35

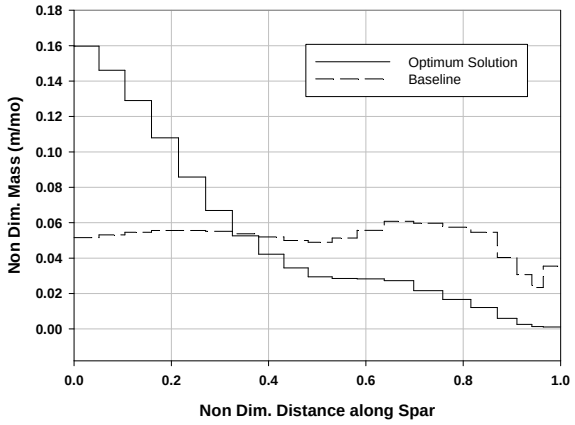

Fig. 6: Spanwise material grading of twenty-segment spar

function fmincon is applied to most smooth objective functions with smooth constraints. It is the most suitable function to the optimization problem of this investigation.

Baseline design: Definition of a baseline design is intended in order to simplify and clarify the effects of changing variables on the objective natural frequencies of different modes of vibrations. Baseline design is a composite box beam with specific variables to which every design variable under investigation is compared. Normalization of design variables is done by dividing each variable by the corresponding one of the baseline design. Thus, actual value of any design variable or natural frequency can be obtained by multiplying the normalized value by that of the baseline design. Figure 5 shows the effect of fiber orientation angle on the bending natural frequencies of a uniform (single segment) box beam. The dimensions of that beam are 40 mm width, 25 mm height, 0.9 mm thickness and 800 mm length. The beam material is unidirectional laminate of 70 vol. % E-glass fiber/epoxy composite with properties given in Table 1 [1]. It is noticed that axially oriented fibers give the maximum bending natural frequencies. These results are in agreement with those obtained by Armanios and Badir [7]. Baseline beam is thus selected to be uniform box beam with unidirectional laminate of E-glass fiber/epoxy with fiber orientation angle (θ=0) and fiber volume fraction of (V_f =0.5). This fiber layup configuration gives maximum natural frequencies for bending modes of vibration (Fig. 5), while maintain moderate structural mass and strength. Dimensions of baseline beam are selected to be appropriate for a typical application such as wind turbine blades. Length of baseline beam is selected to be (L_o = 7.5 m), height is (h_o=150 mm), width is (w_o =300 mm) and wall thickness is (t_o=10 mm). Mass of the baseline beam is (m_o=122.55 kg). Natural frequencies of the cantilevered baseline beam under consideration are given in Table 2.

Optimum design solutions: For a multiple-segment spar, with each segment built up of single laminate walls, several cases were studied by increasing the number of segments in each case until reaching convergent values of natural frequencies at a number of 20 segments. As the number of segments increases the total run time of the computer program increases. The non-dimensional optimum design solution for the spar with 20 segments is given by:

$$[X_{opt}] = \begin{bmatrix} 0.0516 & 0.0531 & 0.0546 & 0.0556 & 0.0556 & 0.0551 & 0.0538 & 0.0520 & 0.0500 & 0.0490 \\ 1.5979 & 1.5270 & 1.4542 & 1.3801 & 1.3060 & 1.2325 & 1.1607 & 1.0914 & 1.0248 & 0.9594 \\ 0 & 0 & 0 & 0 & 0 & 0 & 0 & 0 & 0 & 0 \\ 0.8 & 0.8 & 0.8 & 0.8 & 0.8 & 0.8 & 0.8 & 0.8 & 0.8 & 0.8 \\ 1.5873 & 1.4730 & 1.3248 & 1.1439 & 0.9550 & 0.7937 & 0.6757 & 0.5963 & 0.5393 & 0.5 \end{bmatrix}$$

$$\begin{bmatrix} 0.0514 & 0.0557 & 0.0608 & 0.0597 & 0.0575 & 0.0546 & 0.0403 & 0.0307 & 0.0234 & 0.0355 \\ 0.8909 & 0.8166 & 0.7396 & 0.6560 & 0.5793 & 0.5065 & 0.3519 & 0.2326 & 0.1490 & 0.1 \\ 0 & 0 & 0 & 0 & 0 & 0 & 0 & 0 & 0 & 0 \\ 0.8 & 0.8 & 0.7739 & 0.6253 & 0.4883 & 0.3304 & 0.3208 & 0.3144 & 0.3009 & 0.2 \\ 0.5 & 0.5 & 0.5 & 0.5 & 0.5 & 0.5 & 0.5 & 0.5 & 0.5 & 0.5 \end{bmatrix} \quad (29)$$

Table 3: Actual dimensions (mm) and natural frequencies of the optimum spar

Seg.	1	2	3	4	5	6	7	8	9	10	11	12	13	14	15	16	17	18	19	20
L	387	398	410	417	417	413	404	390	374	368	386	417	456	448	432	409	302	230	176	266
h	240	229	218	207	196	185	174	164	154	144	134	123	110	98	87	76	53	35	22	15
t	15.9	14.7	13.2	11.4	9.6	7.9	6.8	6	5.4	5	5	5	5	5	5	5	5	5	5	5
	VB1 = 10.14 Hz						VB2 = 30.2 Hz							VB3 = 55 Hz						
	HB1 = 17.6 Hz						HB2 = 52.5 Hz							HB3 = 95.6 Hz						

Table 4: Comparison of mass (kg) and natural frequencies (Hz) between baseline and optimum designs

Design	Mass	VB1	VB2	VB3	HB1	HB2	HB3
Baseline	122.55	2.80	17.55	49.14	4.86	30.5	85.35
Optimum	122.55	10.14	30.20	55.00	17.60	52.5	95.60
Change %	0.00	262.00	72.00	12.00	262.00	72.0	12.00

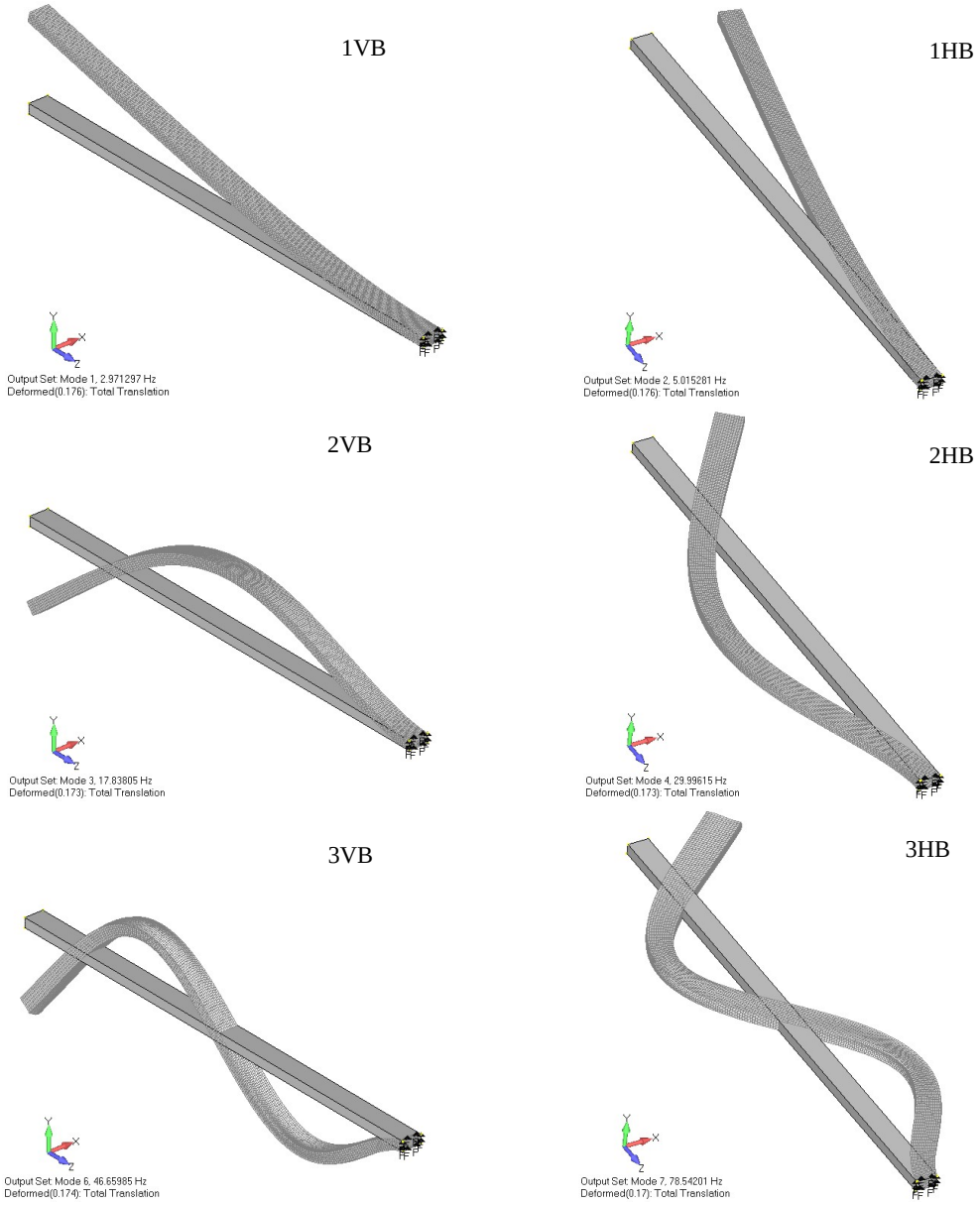

Fig. 7: Mode shapes and natural frequencies for vertical and horizontal bending vibration of the baseline design

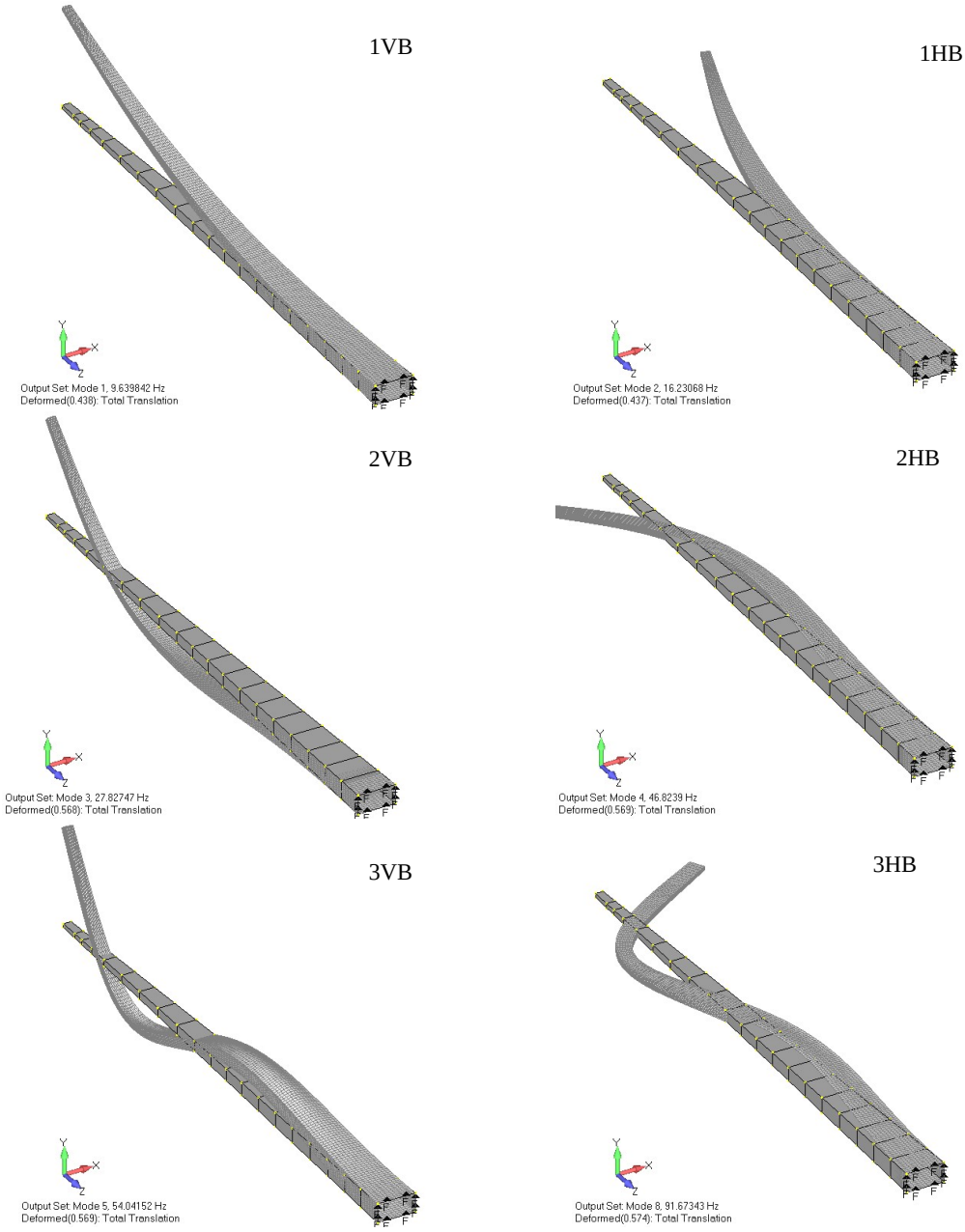

Fig. 8: Mode shapes and natural frequencies for vertical and horizontal bending vibration of the optimum design

Non-dimensional bending natural frequencies of such a spar are 3.62, 1.72 and 1.12 for first, second and third modes of vibration respectively. Mass of that spar is equal to that of the baseline beam. Actual dimensions and natural frequencies of the optimum spar are given in Table 3. It is obvious that a considerable increase in all frequencies had been achieved as compared to the original baseline design (Table 4). It can also be seen that good beam design for flapping dynamics should have smaller wall thickness in the outboard portion of the blade where the strength constraints are active. This completely differs from the traditional designs of keeping wall thickness constant along the beam. The optimization process recommended the segments located inboard to have high wall thickness and high fiber content. The spanwise variation in the height of each segment of the beam is always restricted by the taper envelope which is the major obstacle in design optimization. Considering now the mass distribution along the spar, that is the main factor in material grading concept. It is known that mass of each segment depends on length, cross section dimensions and fiber

Table 5: Comparison of natural frequencies between analytical and FEM results in Hz

	Baseline design			Optimum design		
Mode	Analytical	FEM	Diff. %	Analytical	FEM	Diff. %
VB1	2.80	2.97	5.7	10.14	9.64	5.0
VB2	17.55	17.84	1.6	30.20	27.83	7.8
VB3	49.14	46.70	5.0	55.00	54.00	1.8
HB1	4.86	5.02	3.2	17.60	16.23	7.8
HB2	30.50	30.00	1.6	52.50	46.82	10.0
HB3	85.35	78.60	7.9	95.60	91.97	4.0

content within that segment. Figure 6 presents the optimum spanwise mass distribution in case of twenty-segment spar. As a general observation, the rate of reducing mass as going from root towards tip is recommended to be higher than that of the baseline design.

Finite element validation: In order to validate the results obtained from the analytical model considered in this investigation, a comparison with finite element results was performed for the baseline and the optimum spar designs. The finite element analysis was conducted by using NX Nastran solver, with the baseline and the optimum designs modeled by using 2700 and 4860 linear laminate plate 4-noded quad elements respectively. Figure 7 and 8 shows mode shapes with the associated natural frequencies for bending vibration of baseline and optimum designs, respectively. The first three natural frequencies of bending vibration obtained by both analytical and finite element methods are compared in Table 5 for both baseline and optimum designs. The agreement between the two methods of prediction is acceptable.

CONCLUSIONS

An efficient mathematical optimization model for enhancing the dynamic performance of thin-walled composite blades with spanwise material grading was developed. The formulation of an optimum design providing high natural frequencies was investigated. Constraints were imposed on the design variables in order to avoid abnormal-shaped optimized configurations. An analytical model was implemented taking into consideration all the design variables such as cross-section dimensions and lamination parameters. The proposed model deals with dimensionless quantities in order to be applicable to thin-walled beams with arbitrary dimensions. Results indicated that the optimization process leads to significant increase of natural frequencies of the optimized spar from 12 to 262% when compared to the reference baseline design without mass change. Finite element model showed a good agreement with the analytical model developed in this study with a variation up to 10%.

REFERENCES

1. Daniel, G. and S.V. Hoa, 2007. Composite Materials Design and Applications. CRC Press.
2. Daneil, I.M. and O. Ishai, 2006. Engineering Mechanics of Composite Materials. Oxford University Press.
3. Berthelot, J.M., 1999. Mechanics of Composite Materials and Structures. Springer.
4. Lipton, R., 2002. Design of functionally graded composite structures in the presence of stress constraints. Int. J. Solids Struct., 39: 2575-2586.
5. Libriscu, L. and K.Y. Maalawi, 2007.Material Grading for Improved Aeroelastic Stability of Composite Wings. Journal of Mechanics of Materials and Structures, 2: 1381-1394.
6. Miyamoto, Y., M. Niino and M. Koizumi, 1997. FGM research programs in Japan-from structural to functional uses. Elsevier Science.
7. Armanios, E.A. and A.M. Badir, 1995. Free Vibration Analysis of Anisotropic Thin-Walled Closed-Sections Beams. American Institute of Aeronautics and Astronautics (AIAA), 33: 1905-1910.
8. Dancila, D.S. and E.A. Armanios, 1998. The Influence of Coupling on The Free Vibration of Anisotropic Thin-Walled Closed-Section Beams. Int. J. Solids Struct., 35: 3105-3119.
9. Durmaz, S. and M.O. Kaya, 2009. Free Vibration of An Anisotropic Thin-Walled Box Beam Under Bending-Torsion Coupling. In the Preceedings of 3rd International Conference On Integrity, Reliability and Failure.
10. Shadmehri, F., H. Haddadpour and M. Kouchakzageh, 2007. Flexural-torsional behaviour of thin-walled composite beams with closed cross-section. Thin Walled Struct, 45: 699-705.

11. Phuong, T. and J. Lee, 2008. Flexural-torsional behavior of thin-walled composite box beams using shear-deformable beam theory. Eng. Struct., 30: 1958-1968.
12. Piovan, M.T., C.P. Filipicha and V.H. Cortínez, 2006. Coupled free vibration of tapered box beams made of composite materials. Mecánica Computacional, 25: 1767-1779.
13. Kargarnovin, M.H. and M. Hashemi, 2012. Free vibration analysis of multilayered composite cylinder consisting fibers with variable volume fraction. Compos. Struct., 94: 931-944.
14. Liu, Y. and D.W. Shu, 2014. Free vibration analysis of exponential functionally graded beams with a single delamination. Composites Part B, 59: 166-172.
15. Reddy, J.N., 2004. Mechanics of Laminated Composite Plates and Shells: Theory and Analysis. CRC Press LLC.
16. Halpin, J.C. and S.W. Tsai, 1969. Effect of Environmental Factors on Composite Materials. Report AFML-TR pp: 67-423.
17. Song, O. and L. Librescu, 2006. Thin-Walled Composite Beams, Theory and Application. Springer.
18. Mihail, B., C. Valentin and D. Costin, 2014. A transfer matrix method for free vibration analysis of Euler-Bernoulli beams with variable cross section. J. Vib. Control, pp: 1-12.
19. Meirovitch, L., 1967. Analytical Methods in Vibrations. The Macmillan Co.
20. Rao, S. and Singiresu, 2009. Engineering Optimization: Theory and Practice. John Wiley & Sons Inc.
21. Kelley, C.T., 1999. Iterative Methods for Optimization. Society for Industrial and Applied Mathematics.
22. Nocedal, J. and J. Stephen, 1999. Numerical Optimization. Springer.